

# Image Sequence Analysis via Partial Differential Equations

PIERRE KORNPORST, RACHID DERICHE

Pierre.Kornprobst@sophia.inria.fr Rachid.Deriche@sophia.inria.fr  
*INRIA, 2004 route des Lucioles, BP 93, 06902 Sophia-Antipolis Cedex, France*

GILLES AUBERT

gaubert@math.unice.fr  
*Laboratoire J.A Dieudonne, UMR n° 6621 du CNRS, 06108 Nice-Cedex 2, France*

*Received ??; Revised ??*

Editors: ??

**Abstract.** This article deals with the problem of restoring and motion segmenting noisy image sequences with a static background. Usually, motion segmentation and image restoration are considered separately in image sequence restoration. Moreover, motion segmentation is often noise sensitive. In this article, the motion segmentation and the image restoration parts are performed in a coupled way, allowing the motion segmentation part to positively influence the restoration part and vice-versa. This is the key of our approach that allows to deal simultaneously with the problem of restoration and motion segmentation. To this end, we propose a theoretically justified optimization problem that permits to take into account both requirements. The model is theoretically justified. Existence and unicity are proved in the space of bounded variations. A suitable numerical scheme based on half quadratic minimization is then proposed and its convergence and stability demonstrated. Experimental results obtained on noisy synthetic data and real images will illustrate the capabilities of this original and promising approach.

**Keywords:** Sequence image restoration, motion segmentation, discontinuity preserving regularization, variational approaches, space of bounded variation

## 1. Introduction

Automatic image sequence restoration is clearly a very important problem. Applications areas include image surveillance, forensic image processing, image compression, digital video broadcasting, digital film restoration, medical image processing, remote sensing ... See, for example, the recent work done within the European projects, fully or in part, involved with this important problem : *AURORA*<sup>1</sup> (Automated Restoration of Film and Video Archives), *NOBLESSE*<sup>2</sup> (Nonlin-

ear Model-Based Analysis and Description of Images for Multimedia Application), *IMPROOFS*<sup>3</sup> (IMage PROcessing Operations for Forensic Support), ... Image sequence restoration is tightly coupled to motion segmentation. It requires to extract moving objects in order to separately restore the background and each moving region along its particular motion trajectory. Most of the work done mainly involves motion compensated temporal filtering techniques with appropriate 2D or 3D Wiener filter for noise suppression, 2D/3D median filtering or more appropri-

ate morphological operators for removing impulsive noise [16, 38, 39, 31, 27, 52, 19, 17]. However, and due to the fact that image sequence restoration is an emerging domain compared to 2D image restoration, the literature is not so abundant than the one related to the problem of restoring just a single image. For example, numerous PDE based algorithms have been recently proposed for noise removal, 2D image enhancement and 2D image restoration in real images with a particular emphasis on preserving the grey level discontinuities during the enhancement/restoration process. These methods, which have been proved to be very efficient, are based on evolving nonlinear partial differential equations (PDE's) (See the work of Alvarez *et al* [4], Aubert *et al.* [8], Chambolle & Lions [21], Chan [14, 67] Cohen [23], Cottet & Germain [24], Kornprobst & Deriche [44, 43, 42], Malladi & Sethian [46], Mumford & Shah [65, 53], Morel [3, 51], Nordström [54], Osher & Rudin [60], Perona & Malik [58], Proesman *et al.* [59], Sapiro *et al.* [20, 61, 62, 12, 63], Weickert [71, 72], You *et al.* [74], ...). This methodology provides several advantages. Firstly, we can justify on a theoretical point of view the model, using the theory of viscosity solutions or the calculus of variations. Secondly, it provides some suitable numerical schemes for which convergence may be proved. Finally, it permits to obtain results of high quality.

It is the aim of this article to consider the important problem of image sequence restoration by applying this PDE based methodology, which has been proved to be very successful in anisotropically restoring images. To our knowledge, few literature exists on the analysis of sequences of images using Partial Differential Equations. However, we mention that this methodology has been previously used in the context of multiscale analysis of movies (see the works of Guichard [35] and Moisan [50]). In all this work, we will assume that the background is static. We recall that the background will be defined as the most often observed part over the sequence. Our goal will be to obtain the motion segmentation and the restored background.

Therefore, considering the case of an image sequence with some moving objects, we have to consider both motion segmentation and image restoration problems. Usually, these two problems

are treated separately in image sequence analysis. However, it is clear that these two problems should be treated simultaneously in order to achieve better results. This is the key of our approach that allows to deal simultaneously with the problem of restoration and motion segmentation.

The organization of the article is as follows.

In Sect. 2, we make some precise recalls about one of our previous approach for denoising a single image [26, 8, 43]. The formalism and the methods introduced will be very useful in the sequel.

Section 3 is then devoted to the presentation of our new approach to deal with the case of noisy images sequences. We formulate the problem into an optimization problem.

The model is theoretically justified in Sect. 4 : we prove the existence and the unicity of the solution to our problem in the space of bounded variation functions.

A suitable algorithm is then proposed in Sect. 5 to approximate numerically the solution. We prove its convergence and its stability.

We propose in Sect. 6 some experimental results obtained on noisy synthetic and real data that will illustrate the capabilities of this new approach.

We conclude in Sect. 7 by recalling the specificities of that work and giving the future developments.

## 2. Restoring a single image

In Sect. 2.1, we recall a classical method in image restoration formulated as a minimization problem [26, 11, 8]. Section 2.2 presents a suitable algorithm called the half quadratic minimization which will also be used in the sequel.

### 2.1. A Classical Approach for Image Restoration

Let  $N(x_1, x_2)$  be a given noisy image defined for  $x = (x_1, x_2) \in \Omega \subset R^2$  which corresponds to the domain of the image.  $\nabla$ . is the gradient operator. We search for the restored image  $I(x_1, x_2)$  as the solution of the following minimization problem :

$$\inf_I \underbrace{\int_{\Omega} (I - N)^2 dx}_{\text{term 1}} + \alpha^r \underbrace{\int_{\Omega} \phi(|\nabla I|) dx}_{\text{term 2}} \quad (1)$$

where  $|\cdot|$  is the usual euclidian norm,  $\alpha^r$  is a constant and  $\phi$  is a function still to be defined. Notice that if  $\phi(t) = t^2$ , we recognize the *Tikhonov-Arsenin* regularization term [68]. How can we interpret this minimization with this choice? In fact, we search for the function  $I$  which will be simultaneously close to the initial image  $N$  and smooth (since we want the gradient as small as possible). However, this method is well known to smooth the image isotropically without preserving discontinuities in intensity. The reason is that with the quadratic function, gradients are too much penalized. One solution to prevent the destruction of discontinuities but allows for isotropically smoothing uniform areas, is to change the above quadratic term. This point have been widely discussed [13, 53, 64, 66, 11, 8]. We refer to [26] for a review. The key idea is that for low gradients, isotropic smoothing is performed, and for high gradient, smoothing is only applied in the direction of the isophote and not across it. This condition can be mathematically formalized if we look at the Euler-Lagrange Equation (2), associated to energy (1) :

$$2(I - N) - \alpha^r \operatorname{div} \left( \frac{\phi'(|\nabla I|)}{|\nabla I|} \nabla I \right) = 0 \quad (2)$$

Notice that Neumann conditions are imposed on the boundaries. Let us concentrate on the divergence term associated to the term 2 of (1). If we note  $\eta = \frac{\nabla I}{|\nabla I|}$ , and  $\xi$  the normal vector to  $\eta$  ( $|\xi| = 1$ ), we can show that [26] :

$$\operatorname{div} \left( \frac{\phi'(|\nabla I|)}{|\nabla I|} \nabla I \right) = \underbrace{\frac{\phi'(|\nabla I|)}{|\nabla I|} I_{\xi\xi}}_{c_\xi} + \underbrace{\phi''(|\nabla I|) I_{\eta\eta}}_{c_\eta} \quad (3)$$

where  $I_{\eta\eta}$  (respectively  $I_{\xi\xi}$ ) denotes the second order derivate in the direction  $\eta$  (respectively  $\xi$ ). It is interesting to notice that most diffusions operators used for image restoration may also be decomposed as the weighted sum of the second directional derivatives  $I_{\xi\xi}$  and  $I_{\eta\eta}$ . We refer to [41] for more details. As for operator (3), if we want a good restoration as described before, we would

like to have the following properties :

$$\lim_{|\nabla I| \rightarrow 0} c_\eta = \lim_{|\nabla I| \rightarrow 0} c_\xi = a_0 > 0 \quad (4)$$

$$\lim_{|\nabla I| \rightarrow \infty} c_\eta = 0 \text{ and } \lim_{|\nabla I| \rightarrow \infty} c_\xi = a_\infty > 0 \quad (5)$$

But it is clear that the two conditions in (5) are incompatible. So, we will only impose for high gradients [26, 11, 8] :

$$\lim_{|\nabla I| \rightarrow \infty} c_\eta = \lim_{|\nabla I| \rightarrow \infty} c_\xi = 0 \quad (6)$$

$$\lim_{|\nabla I| \rightarrow \infty} \left( \frac{c_\eta}{c_\xi} \right) = 0$$

Many functions  $\phi$  have been proposed in the literature that comply with the conditions (4) and (6) (see [26]). From now on,  $\phi$  will be a convex function with linear growth at infinity which verifies conditions (4) and (6). For instance, a possible choice could be the hypersurface minimal function

$$\phi(t) = \sqrt{1+t^2} - 1 \quad (7)$$

In that case, existence and unicity of problem (1) has recently been shown in the Sobolev space  $W^{1,1}(\Omega)$ [11] (See also [69]).

## 2.2. The Half Quadratic Minimization

Solving directly the minimization problem (1) by solving directly its Euler Lagrange equation (2), is something hard because this equation is highly non linear.

To overcome the difficulty, the key idea is to introduce a new functional which, although defined over an extended domain, has the same minimum in  $I$  and can be manipulated with linear algebraic methods. The method is based on the half quadratic minimization theorem, inspired from Geman and Reynolds [30]. The general idea is that under some hypotheses on  $\phi$  (mainly  $\phi(\sqrt{t})$  concave), we can write it as an infimum :

$$\phi(t) = \inf_d (dt^2 + \psi(d)) \quad (8)$$

where  $d$  will be called the *dual variable* associated to  $x$ , and where  $\psi(\cdot)$  is a convex and decreasing function. We refer to the Appendix A for more details. We can verify that the function proposed in (7) can be written as in (8). Consequently, the problem (1) is now to find  $I$  and its dual variable

$d_I$  minimizing the functional  $\mathcal{F}(I, d_I)$  defined by :

$$\mathcal{F}(I, d_I) = \int_{\Omega} (I - N)^2 dx + \alpha^r \int_{\Omega} (d_I |\nabla I|^2 + \psi(d_I)) dx \quad (9)$$

It is easy to check that for a fixed  $I$ , the functional  $\mathcal{F}$  is convex in  $d_I$  and for a fixed  $d_I$ , it is convex in  $I$ . These properties are used to perform the algorithm which consists in minimizing alternatively in  $I$  and  $d_I$  :

$$I^{n+1} = \underset{I}{\operatorname{argmin}} \quad \mathcal{F}(I, d_I^n) \quad (10)$$

$$d_I^{n+1} = \underset{d_I}{\operatorname{argmin}} \quad \mathcal{F}(I^{n+1}, d_I) \quad (11)$$

To perform each minimization, we simply solve the Euler-Lagrange equations, which can be written as

$$I^{n+1} - N - \alpha^r \operatorname{div}(d_I^n \nabla I^{n+1}) = 0 \quad (12)$$

$$d_I^{n+1} = \frac{\phi'(|\nabla I^{n+1}|)}{2|\nabla I^{n+1}|} \quad (13)$$

with discretized Neumann conditions at the boundaries. Notice that (13) gives explicitly  $d_I^{n+1}$  while for (12), for a fixed  $d_I^n$ ,  $I^{n+1}$  is the solution of a linear equation. After discretizing in space, we have that  $(I_{i,j}^{n+1})_{(i,j) \in \Omega}$  is solution of a linear system which is solved iteratively by the Gauss-Seidel method for example. We refer to the Appendix B for more details about the discretization of the divergence operator. We also mention that the convergence of the algorithm has been proved [69].

### 3. Dealing with Noisy Images Sequences

Let  $N(x_1, x_2, t)$  denotes the noisy images sequence for which the background is assumed to be static. A simple moving object detector can be obtained using a thresholding technique over the *inter-frame difference* between a so-called *reference image* and the image being observed. Decisions can be taken independently point by point [73]. More complex approaches can also be used [55, 57, 56, 1, 36, 45, 16, 38, 39, 31, 27, 52]. However, in our application, we are not just dealing with a motion segmentation problem neither just a restoration problem. In our case, the so-called *reference image* is built at the same time while

observing the image sequence. Also, the motion segmentation and the restoration are done in a coupled way, allowing the motion segmentation part to positively influence the restoration part and vice-versa. This is the key of our approach that allows to deal simultaneously with the problem of restoration and motion segmentation.

We first consider that the data is continuous in time. This permits us to present the optimization problem we want to study (Sect. 3.1). In Sect. 3.2, we rewrite the problem when the sequence is given only by a finite set of images. This leads to the Problem 2.

#### 3.1. An Optimization Problem

Let  $N(x_1, x_2, t)$  denotes the noisy images sequence for which the background is assumed to be static. Let us describe the unknown functions and what we would like them ideally to be :

- (i)  $B(x_1, x_2)$ , the restored background,
- (ii)  $C(x_1, x_2, t)$ , the sequence which will indicate the moving regions. Typically, we would like that  $C(x_1, x_2, t) = 0$  if the pixel  $(x_1, x_2)$  belongs to a moving object at time  $t$ , and 1 otherwise.

Our aim is to find a functional depending on  $B(x_1, x_2)$  and  $C(x_1, x_2, t)$  so that the minimizers verify previous statements. We propose to solve the following problem :

**Problem 1.** Let  $N(x_1, x_2, t)$  the given noisy image sequence. We search for the restored background  $B(x_1, x_2)$  and the motion segmented sequence  $C(x_1, x_2, t)$  as the solution of the following minimization problem :

$$\inf_{B,C} \left( \underbrace{\int_t \int_{\Omega} C^2 (B - N)^2 dx dt}_{\text{term 1}} + \alpha_c \underbrace{\int_t \int_{\Omega} (C - 1)^2 dx dt}_{\text{term 2}} + \alpha_b^r \int_{\Omega} \phi_1(|\nabla B|) dx + \alpha_c^r \int_t \int_{\Omega} \phi_2(|\nabla C|) dx dt \right) \quad (14)$$

term 3

where  $\phi_1$  and  $\phi_2$  are convex functions that comply conditions (4) and (6), and  $\alpha_c, \alpha_b^r, \alpha_c^r$  are positive constants. We will specify later the spaces over



which the minimization runs.

Getting the minimum of the functional means that we want each term to be small, having in mind the phenomena of the compensations.

The **term 3** is a regularization term. Notice that the functions  $\phi_1, \phi_2$  have been chosen as in Sect. 2 so that discontinuities may be kept.

If we consider the **term 2**, this means that we want the function  $C(x_1, x_2, t)$  to be close to one. In our interpretation, this means that we give a preference to the background. This is physically correct since the background is visible most of the time. However, if the data  $N(x_1, x_2, t)$  is too far from the supposed background  $B(x_1, x_2)$  at time  $t$ , then the difference  $(B(x_1, x_2) - N(x_1, x_2, t))^2$  will be high, and to compensate this value, the minimization process will force  $C(x_1, x_2, t)$  to be zero. Therefore, the function  $C(x_1, x_2, t)$  can be interpreted as a motion detection function. Moreover, when searching for  $B(x_1, x_2)$ , we will not take into account  $N(x_1, x_2, t)$  if  $C(x_1, x_2, t)$  is small (**term 1**). This exactly means that  $B(x_1, x_2)$  will be the restored image of the static background.

**Remark : What about regularizing in time the functions?** As we can notice, the **term 3** is a spatial smoothing term and we may suggest to add some temporal smoothing for the sequence  $C$ . However, there are two difficulties to keep in mind:

- the sequence has to be well sampled in time. This temporal regularization term will have no real interpretation in cases of images taken at very large times (as it can be the case in video-surveillance).

- In the same spirit as before, the discretization of the regularization operator (in time) will be hard because it will depend strongly on the kind of movement in the sequence. In fact this kind of regularization is, in some way, equivalent to find the optical flow, which we wanted to avoid. We can think that this term could be useful and well discretized in a multiscale approach."

### 3.2. The Temporal Discretized Problem

In fact, we have only a finite set of images. Consequently, we are going to rewrite the Problem 1, taking into account that the sequence  $N(x_1, x_2, t)$  is represented during a finite time by  $T$  images noted  $N_1(x_1, x_2), \dots, N_T(x_1, x_2)$ . The Problem 1 becomes :

**Problem 2.** Let  $N_1, \dots, N_T$  be the noisy sequence. We search for  $B$  and  $C_1, \dots, C_T$  as the solution of the following minimization problem :

$$\begin{aligned} \inf_{B, C_1, \dots, C_T} & \left( \underbrace{\sum_{h=1}^T \int_{\Omega} C_h^2 (B - N_h)^2 dx}_{\text{term 1}} \right. \\ & + \underbrace{\alpha_c \sum_{h=1}^T \int_{\Omega} (C_h - 1)^2 dx}_{\text{term 2}} \\ & \left. + \underbrace{\alpha_b^r \int_{\Omega} \phi_1(|\nabla B|) dx + \alpha_c^r \sum_{h=1}^T \int_{\Omega} \phi_2(|\nabla C_h|) dx}_{\text{term 3}} \right) \end{aligned} \quad (15)$$

Before going further, one may be interested in the link between this method and the variational method developed for image restoration in section 2. To this end, let us consider a sequence of the same noisy image. More generally, we can consider a sequence of the same static image corrupted with different noises. If we admit the interpretation of the functions  $C_h$ , we will have  $C_h \equiv 1$ . After few computations, (15) may be re-written :

$$\inf_B \left( \int_{\Omega} \left( B - \frac{1}{T} \sum_{h=1}^T N_h \right)^2 dx + \frac{\alpha_b^r}{T} \int_{\Omega} \phi_1(|\nabla B|) dx \right)$$

Consequently, if we observe the energy (1) proposed for the image restoration problem, we can consider  $B$  as the restored version of the mean in time of the sequence. Notice that if the sequence is simply  $T$  times the same image, both methods correspond exactly. Therefore, this model devoted to sequences of images can be considered as a natural extension of the previous one for single image restoration.

Now that we have justified the proposed model, let us prove that it is mathematically well posed. It is the purpose of the next section.

#### 4. A Rigorously Justified Approach in The Space of Bounded Variations

Section 4.1 presents the mathematical background of our problem : the space of bounded variations which is suitable to most problems in vision [60, 22]. Roughly speaking, the idea is to generalize the classical Sobolev space  $W^{1,1}(\Omega)$  so that discontinuities along hypersurfaces may be considered. After having precisely specified the problem in Sect. 4.2, we first prove the existence of a solution in a constrained space (See Sect. 4.3). Using this result, we finally prove the existence and the unicity of a solution over the space in bounded variations in Sect. 4.4.

##### 4.1. The Space $BV(\Omega)$ : a Short Overview

In this section we only recall main notations and definitions. We refer to [2, 28, 33, 29, 75] for the complete theory.

Let  $\Omega$  be a bounded open set in  $R^N$ , with Lipschitz-regular boundary  $\partial\Omega$ . We denote by  $\mathcal{L}^N$  or  $dx$  the  $N$ -Lebesgue dimensional measure in  $R^N$  and by  $\mathcal{H}^\alpha$  the  $\alpha$ -dimensional Hausdorff measure. We also set  $|E| = \mathcal{L}^N(E)$ , the Lebesgue measure of a measurable set  $E \subset R^N$ .  $\mathcal{B}(\Omega)$  denotes the family of the Borel subsets of  $\Omega$ . We will respectively denote the strong, the weak and weak\* convergences in a space  $V(\Omega)$  by  $\xrightarrow{V(\Omega)}$ ,  $\xrightarrow{V(\Omega)}$ ,  $\xrightarrow{V(\Omega)^*}$ .

Spaces of vector valued functions will be noted by bold characters.

Working with images requires that the functions that we consider can be discontinuous along curves. This is impossible with classical Sobolev spaces such as  $W^{1,1}(\Omega)$ . This is why we need to use the space of bounded variations (noted  $BV(\Omega)$ ) defined by :

$$BV(\Omega) = \left\{ u \in L^1(\Omega); \sup_{\varphi} \int_{\Omega} u \operatorname{div}(\varphi) dx < \infty : \right. \\ \left. \varphi \in C_0^1(\Omega)^2, |\varphi|_{\infty} \leq 1 \right\}$$

where  $C_0^1(\Omega)$  is the set of differentiable functions with compact support in  $\Omega$ . We will note :

$$|Du|(\Omega) = \sup \left\{ \int_{\Omega} u \operatorname{div}(\varphi) dx : \varphi \in C_0^1(\Omega)^2, |\varphi|_{\infty} \leq 1 \right\}$$

If  $u \in BV(\Omega)$  and  $Du$  is the gradient in the sense of distributions, then  $Du$  is a vector valued Radon measure and  $|Du|(\Omega)$  is the total variation of  $Du$  on  $\Omega$ . The set of Radon measure is noted  $\mathcal{M}(\Omega)$

The product topology of the strong topology of  $L^1(\Omega)$  for  $u$  and of the weak\* topology of measures for  $Du$  will be called the weak\* topology of  $BV$ , and will be denoted by  $BV - w^*$ .

$$u^n \xrightarrow{BV-w^*} u \iff \begin{cases} u^n \xrightarrow{L^1(\Omega)} u \\ Du^n \xrightarrow{\mathcal{M}(\Omega)^*} Du \end{cases} \quad (16)$$

We recall that every bounded sequence in  $BV(\Omega)$  admits a subsequence converging in  $BV - w^*$ .

We define the approximate upper limit  $u^+(x)$  and the approximate lower limit  $u^-(x)$  by :

$$u^+(x) = \inf \left\{ t \in [-\infty, +\infty] : \lim_{\rho \rightarrow 0^+} \frac{|u > t| \cap B_{\rho}(x)}{\rho^N} = 0 \right\} \\ u^-(x) = \sup \left\{ t \in [-\infty, +\infty] : \lim_{\rho \rightarrow 0^+} \frac{|u < t| \cap B_{\rho}(x)}{\rho^N} = 0 \right\}$$

where  $B_{\rho}(x)$  is the ball of center  $x$  and radius  $\rho$ . We denote by  $S_u$  the jump set, that is to say the complement of the set of Lebesgue points, *i.e.* the set of points  $x$  where  $u^+(x)$  is different  $u^-(x)$ , namely :

$$S_u = \{x \in \Omega / u^-(x) < u^+(x)\}.$$

After choosing a normal  $n_u(x)$  ( $x \in S_u$ ) pointing toward the largest value of  $u$ , we recall the following decompositions ([5] for more details):

$$Du = \nabla u \cdot \mathcal{L}_N + C_u + (u^+ - u^-)n_u \cdot \mathcal{H}_{S_u}^{N-1} \quad (17)$$

where  $\nabla u$  is the density of the absolutely continuous part of  $Du$  with respect to the Lebesgue measure,  $\mathcal{H}_{S_u}^{N-1}$  is the Hausdorff measure of dimension  $N - 1$  restricted to the set  $S_u$  and  $C_u$  is the Cantor part. We then recall the definition of a convex function of measures. We refer to the works of Goffman-Serrin [34] and Demengel-Temam [25] for more details. Let  $\phi$  be convex and finite on  $R$  with linear growth at infinity. Let  $\phi^\infty$  be the

asymptote (or recession) function :

$$\phi^\infty(z) := \lim_{t \rightarrow \infty} \frac{\phi(tz)}{t} \in [0; +\infty),$$

then for  $u \in BV(\Omega)$ , using classical notations, we define

$$\int_{\Omega} \phi(Du) = \int_{\Omega} \phi(|\nabla u|) dx + \phi^\infty(1) \int_{\Omega \setminus S_u} |C_u| + \phi^\infty(1) \int_{S_u} (u^+ - u^-) d\mathcal{H}^{N-1} \quad (18)$$

We finally mention that this function is lower semi-continuous for the  $BV - w_\star$ -topology.

#### 4.2. Setting the problem

Let us recall the problem. Notice that the derivatives will be now considered as distributional derivatives. Consequently, the problem is to minimize over  $BV(\Omega)^{T+1}$  the functional  $E$  defined by

$$\begin{aligned} E(B, C_1, \dots, C_T) = & \quad (19) \\ & \sum_{h=1}^T \int_{\Omega} C_h^2 (B - N_h)^2 dx + \alpha_c \sum_{h=1}^T \int_{\Omega} (C_h - 1)^2 dx \\ & + \alpha_b \int_{\Omega} \phi_1(DB) + \alpha_c \sum_{h=1}^T \int_{\Omega} \phi_2(DC_h) \end{aligned}$$

We recall that the regularization terms are interpreted as convex functions of measures (see (18)). The precise hypotheses on the functions  $(\phi_j)_{j=1,2}$  are :

$$\begin{aligned} \phi_j : R \rightarrow R^+ \text{ is an even and strictly convex} \\ \text{function, nondecreasing on } R^+ \text{ and there} \\ \text{exist constants } c > 0 \text{ and } b \geq 0 \text{ such that} \\ cx - b \leq \phi_j(x) \leq cx + b \text{ for all } x \in R^+ \\ \phi(0) = 0, \quad \phi_j^\infty(1) = 1 \end{aligned} \quad (20) \quad (21)$$

As for the data  $(N_h)_{h=1..T}$ , we will assume that :

$$N_h \in BV(\Omega) \cap L^\infty(\Omega) \quad \forall h = 1..T \quad (22)$$

and we will denote  $m_N$  and  $M_N$  the constants defined by :

$$\begin{cases} m_N = \operatorname{ess\,inf}_{h \in [0..T], (x_1, x_2) \in \Omega} N_h(x_1, x_2) \\ M_N = \operatorname{ess\,sup}_{h \in [0..T], (x_1, x_2) \in \Omega} N_h(x_1, x_2) \end{cases} \quad (23)$$

where *ess - inf* (resp. *ess - sup*) is the essential infimum (resp. supremum).

#### 4.3. Existence of a solution in a constrained space

Let us consider the problem :

$$\inf_{(B, C_1, \dots, C_T) \in BV(\Omega)^{T+1}} E(B, C_1, \dots, C_T) \quad (24)$$

Let  $(B^n, C_1^n, \dots, C_T^n) \in BV(\Omega)^{T+1}$  be a minimizing sequence of  $E$ . Thanks to the property (20), one may bound the derivatives of  $B$  and  $C_h$ , and the second term of  $E$  (see (19)) permits us to obtain a bound for  $C_h$ . However, nothing can be said about the norm of  $B$  because of the product in the first term of  $E$  (functions  $C_h$  may be zero).

To overcome this difficulty, let us introduce the restricted space  $\bar{\mathcal{E}}(\Omega)$  defined by :

$$\begin{aligned} \bar{\mathcal{E}}(\Omega) = \{ (B, C_1, \dots, C_T) \in BV(\Omega)^{T+1} \text{ such that:} \\ m_N \leq B \leq M_N \text{ a.e. and } 0 \leq C_h \leq 1 \text{ a.e. } \forall h \} \end{aligned} \quad (25)$$

Then, we have the following theorem :

**Theorem 1.** *Given a sequence of images  $N_h$  verifying (22)-(23), the minimization problem :*

$$\inf_{(B, C_1, \dots, C_T) \in \bar{\mathcal{E}}(\Omega)} E(B, C_1, \dots, C_T) \quad (26)$$

where  $\phi_j$  verify (20)-(21), admits a solution in the set  $\bar{\mathcal{E}}(\Omega)$ .

**Proof:** The proof of this theorem is based on classical arguments. As mentioned at the beginning of this section, the idea is to bound uniformly a minimizing sequence, extract a converging subsequence and pass to the limit. Notice that working on this restricted space permits to obtain a uniform bound for  $B$ . We refer to [10] for the complete proof.  $\square$

#### 4.4. Existence and unicity of a solution over $BV(\Omega)$

The previous theorem establishes the existence of a solution on a restricted space. However, this result is not satisfying because working in a constrained space is not easy to handle because

the optimality conditions are inequations and not equations. In fact, even if these constraints are natural (with regard to the interpretation of the variables), we would like to avoid them. This is the aim of Theorem 2 but we first need a preliminary result :

**Lemma 1.** *Let  $u \in BV(\Omega)$ ,  $\phi$  a function verifying hypotheses (20)-(21), and  $\varphi_{\alpha,\beta}$  the cut-off function defined by :*

$$\varphi_{\alpha,\beta}(x) = \begin{cases} \alpha & \text{if } x \leq \alpha \\ x & \text{if } \alpha \leq x \leq \beta \\ \beta & \text{if } x \geq \beta \end{cases} \quad (27)$$

Then we have :

$$\int_{\Omega} \phi(D\varphi_{\alpha,\beta}(u)) \leq \int_{\Omega} \phi(Du)$$

This Lemma is very intuitive, however we have to deal with distributional derivatives and functions of bounded variation. Consequently, we have to deal with jump sets and Cantor parts. We refer to the Appendix C where the complete proof is sketched.

Using this Lemma, we can state the following result :

**Theorem 2.** *Under hypotheses (20)-(21) and (22)-(23), the minimization problem :*

$$\inf_{(B,C_1,\dots,C_T) \in BV(\Omega)^{T+1}} E(B, C_1, \dots, C_T) \quad (28)$$

admits a solution in  $BV(\Omega)^{T+1}$ . If moreover :

$$\alpha_C \geq 3(M_N - m_N)^2 \quad (29)$$

where the constants  $m_N, M_N$  are defined by (23), then the solution is unique.

**Proof:** Existence is proved showing that the minimization problem (26) over  $\bar{\mathcal{E}}(\Omega)$  is equivalent to the same problem posed over  $BV(\Omega)^{T+1}$ , that is to say without any constraint (this is a di-

rect consequence of Lemma 1). This remark will permit us to prove the existence of a solution.

As for unicity, the difficulty comes from the apparent non convexity of the function :

$$\begin{aligned} & (B, C_1, \dots, C_T) \\ & \quad \downarrow \\ & \sum_{h=1}^T C_h^2 (B - N_h)^2 + \alpha_C \sum_{h=1}^T (C_h - 1)^2 \end{aligned}$$

with respect to all variables (Notice that it is convex with respect to each variable). However, if  $\alpha_C$  is large enough, we prove that this functional is convex over  $\bar{\mathcal{E}}$  which permits to conclude.

We refer to [10] for the complete proof.  $\square$

This theorem is important since it permits to consider the minimization problem over all  $BV(\Omega)^{T+1}$  without any constraint. On a numerical point of view, this remark will be also important since we will not have to handle with Lagrange multipliers. We can also remark that the condition (29) is in fact natural : it means that the background must be sufficiently taken into account.

## 5. The Minimization Algorithm

In the preceding section, we saw that there was a unique solution in  $BV(\Omega)^{T+1}$  of the minimization problem (28). The aim of this section is to propose a suitable algorithm to approximate numerically this solution.

Before beginning, we would like to insist on the fact that working numerically with  $BV(\Omega)$  is something hard. Firstly, we cannot write Euler-Lagrange equations. Anzellotti [7] proposes an extension of Euler-Lagrange equation but they are variational inequalities. In an image restoration background, Vese [69] gives a characterisation of the solution using a dual formulation. However, both of them cannot be used, for the time being, numerically.

Secondly, discretizing directly functions in  $BV(\Omega)$  is still an opened question. For these reasons, we propose an algorithm with two steps :

- Section 5.1 : we define a functional  $E_\epsilon$  on a more regular space. We show that the associated minimization problem admits a unique solution in  $W^{1,2}(\Omega)^{T+1}$  (noted  $(B_\epsilon, C_{1\epsilon}, \dots, C_{T\epsilon})$ ), and

that the functional  $E_\epsilon$   $\Gamma$ -converges to  $E$  for the  $L^2$ -strong topology (We refer to [32, 47] for more details about the notion of  $\Gamma$ -convergence). Consequently,  $(B_\epsilon, C_{1\epsilon}, \dots, C_{T\epsilon})$  will converge for the  $L^2$ -strong topology to the unique solution of the initial problem.

- Section 5.2 : For a fixed  $\epsilon$ , we are going to construct a sequence  $(B^n, C_1^n, \dots, C_T^n)$  converging to  $(B_\epsilon, C_{1\epsilon}, \dots, C_{T\epsilon})$  for the  $L^2$ -strong topology. It will be found as a minimizing sequence of an extended functional. This part usually referenced as the half quadratic minimization.

Consequently, we are able to construct a sequence  $(B^n, C_1^n, \dots, C_T^n)$  converging to the unique minimum of the functional  $E$  for the  $L^2$ -strong topology. We will end this section by presenting in section 5.3 the precise discretized algorithm. Its stability will be proved using the fixed point theorem.

### 5.1. A Quadratic Approximation

We first extend an idea developed in [21]. For a function  $f$  having hypotheses (20)-(21), we define the odd function  $f_\epsilon$  by :

$$f_\epsilon(t) = \begin{cases} \frac{f'(\epsilon)}{2\epsilon}t^2 + f(\epsilon) - \frac{\epsilon f'(\epsilon)}{2} & \text{if } 0 \leq t \leq \epsilon \\ f(t) & \text{if } \epsilon \leq t \leq 1/\epsilon \\ \frac{\epsilon f'(1/\epsilon)}{2}t^2 + f(1/\epsilon) - \frac{f'(1/\epsilon)}{2\epsilon} & \text{if } t \geq 1/\epsilon \end{cases} \quad (30)$$

We observe that for  $\epsilon > 0$ ,  $f_\epsilon \geq f$  and for all  $t$ , we have :  $\lim_{\epsilon \rightarrow 0} f_\epsilon(t) = f(t)$ . Using this definition, let us denote by  $\phi_{1,\epsilon}$  and  $\phi_{2,\epsilon}$  the two functions associated to  $\phi_1$  and  $\phi_2$ . We then define the function  $E_\epsilon$  by :

$$E_\epsilon : BV(\Omega)^{T+1} \rightarrow R \quad (31)$$

$$E_\epsilon(B, C_1, \dots, C_T) = \begin{cases} \sum_{h=1}^T \int_{\Omega} C_h^2 (B - N_h)^2 dx + \alpha_c \sum_{h=1}^T \int_{\Omega} (C_h - 1)^2 dx \\ + \alpha_b^r \int_{\Omega} \phi_{1,\epsilon}(|\nabla B|) dx + \alpha_c^r \sum_{h=1}^T \int_{\Omega} \phi_{2,\epsilon}(|\nabla C_h|) dx \\ \text{if } (B, C_1, \dots, C_T) \in W^{1,2}(\Omega)^{T+1} \\ +\infty \text{ otherwise} \end{cases}$$

Then, using same ideas than for Theorem 2, we can prove that there exists a solution in  $W^{1,2}(\Omega)^{T+1}$  of the problem :

$$\inf_{(B, C_1, \dots, C_T) \in W^{1,2}(\Omega)^{T+1}} E_\epsilon(B, C_1, \dots, C_T) \quad (32)$$

If moreover :

$$\alpha_c \geq 3(M_N - m_N)^2 \quad (33)$$

where the constants  $m_N, M_N$  are defined by (23), then the solution is unique. We will denote by  $(B_\epsilon, C_{1\epsilon}, \dots, C_{T\epsilon})$  the unique minimizer. We have the following proposition :

**Proposition 1.** *The sequence of functionals  $E_\epsilon$   $\Gamma$ -converges to the functional  $E$  for the  $L^{2^{T+1}}$ -strong topology as  $\epsilon$  goes to zero. The sequence of the unique minimum of  $E_\epsilon$ , noted  $(B_\epsilon, C_{1\epsilon}, \dots, C_{T\epsilon})$ , converges in  $L^{2^{T+1}}$ -strong to the unique minimum of  $E$ .*

**Proof:** By construction, the sequence  $E_\epsilon$  is a decreasing sequence converging pointwisely to the functional  $\tilde{E}$  defined by :

$$\tilde{E} : \mathbf{BV}(\Omega) \rightarrow R$$

$$\tilde{E}(B, C_1, \dots, C_T) = \begin{cases} E(B, C_1, \dots, C_T) \\ \text{if } (B, C_1, \dots, C_T) \in \mathbf{W}^{1,2}(\Omega)^{T+1} \\ +\infty \text{ otherwise} \end{cases}$$

Thanks to [47] (proposition 5.7), we can deduce that  $E_\epsilon$   $\Gamma$ -converges to the lower semi continuous envelope of  $\tilde{E}$  (for the  $L^{2^{T+1}}$ -strong topology) noted  $R(E)$ . We then show that in fact  $R(E) = E$  using some compacity results developed for instance in [25, 15].  $\square$

### 5.2. An extension using dual variables

Let  $(B_\epsilon, C_{1\epsilon}, \dots, C_{T\epsilon})$  be the unique minimum of the functional  $E_\epsilon$  over  $W^{1,2}(\Omega)^{T+1}$ . For a fixed  $\epsilon$ , our aim is to approximate it. To this end, we need the result recalled in the Appendix A and already used for the image restoration problem (see Sect. 2.2) : let us apply Theorem 3 to the functions  $\phi_{1,\epsilon}$  and  $\phi_{2,\epsilon}$  which fulfil desired hypotheses (Typically  $\phi_{i,\epsilon}(\sqrt{t})$  are concave). We will denote by  $\Psi_{1,\epsilon}$  and  $\Psi_{2,\epsilon}$  the associated functions

$\Psi$ . We then define the functional  $E_\epsilon^d$  defined over  $(W^{1,2}(\Omega) \times L^2(\Omega)) \times W^{1,2}(\Omega)^T \times L^2(\Omega)^T$  by :

$$\begin{aligned} E_\epsilon^d(B, d_B, C_1, \dots, C_T, d_{C_1}, \dots, d_{C_T}) = & \quad (34) \\ & \sum_{h=1}^T \int_{\Omega} [C_h^2 (B - N_h)^2 + \alpha_c (C_h - 1)^2] dx \\ & + \alpha_b^r \int_{\Omega} [d_B |\nabla B|^2 + \Psi_{1,\epsilon}(d_B)] dx \\ & + \alpha_c^r \sum_{h=1}^T \int_{\Omega} [d_{C_h} |\nabla C_h|^2 + \Psi_{2,\epsilon}(d_{C_h})] dx \end{aligned}$$

where we have introduced the variables  $d_B, d_{C_1}, \dots, d_{C_T}$  associated to  $B, C_1, \dots, C_T$  respectively. To minimize the functional  $E_\epsilon^d$ , the idea is to minimize successively with respect to each variable : given the initial conditions  $(B^0, d_B^0, C_h^0, d_{C_h}^0)$ , we iteratively solve the following system :

$$B^{n+1} = \operatorname{argmin}_{B \in W^{1,2}(\Omega)} E_\epsilon^d(B, d_B^n, C_h^n, d_{C_h}^n) \quad (35)$$

$$d_B^{n+1} = \operatorname{argmin}_{d_B \in L^2(\Omega)} E_\epsilon^d(B^{n+1}, d_B, C_h^n, d_{C_h}^n) \quad (36)$$

$$C_h^{n+1} = \operatorname{argmin}_{C_h \in W^{1,2}(\Omega)} E_\epsilon^d(B^{n+1}, d_B^{n+1}, C_h, d_{C_h}^n) \quad (37)$$

$$d_{C_h}^{n+1} = \operatorname{argmin}_{d_{C_h} \in L^2(\Omega)} E_\epsilon^d(B^{n+1}, d_B^{n+1}, C_h^{n+1}, d_{C_h}) \quad (38)$$

Equalities (37)-(38) are written for  $h = 1..T$ . Notice that the order of the minimization procedure is not important for all the results presented below. The way to obtain each variable like described in (35) to (38) consists in solving the associated Euler-Lagrange equations. As we will see in section 5.3, the dual variables  $d_B^{n+1}$  and  $(d_{C_h}^{n+1})_{h=1..T}$  are given explicitly, while  $B^{n+1}$  and  $(C_h^{n+1})_{h=1..T}$  are solutions of linear systems. Anyway, before going further, we need to know more about the convergence of this algorithm : does it converges and does  $(B^n, C_1^n, \dots, C_T^n)$  approximates  $(B_\epsilon, C_{1\epsilon}, \dots, C_{T\epsilon})$ ? This is the purpose of the following proposition :

**Proposition 2.** *Let  $(B^0, d_B^0, C_h^0, d_{C_h}^0)$  be the initial condition in  $W^{1,2}(\Omega)^{T+1}$ . Then the sequence defined by the system (35)-(36)-(37)-(38) is convergent in  $L^2(\Omega)^{T+1}$ -strong. Moreover, the sequence  $(B^n, C_1^n, \dots, C_T^n)$  converges in*

$L^2(\Omega)^{T+1}$ -strong to the unique minimum of  $E_\epsilon$  in  $W^{1,2}(\Omega)^{T+1}$ , that is to say  $(B_\epsilon, C_{1\epsilon}, \dots, C_{T\epsilon})$ .

**Proof:** The basis of the proof is to write the variational optimality conditions associated to each step and to pass to the limit into them. To this end we needed some results about non-linear elliptic equations [48, 49] and we used a trick of Minty (see for instance [18, 21]). For more details, we refer to [21, 9, 40] where such kind of ideas have been developed.  $\square$

### 5.3. The discretized algorithm

Let us write explicitly the equations that the system (35)-(36)-(37)-(38) implies. Starting from an initial estimate  $(B^0, d_B^0, C_h^0, d_{C_h}^0)$ , the equations that will be solved are the following :

$$\sum_{h=1}^T C_h^{n2} (B^{n+1} - N_h) - \alpha_b^r \operatorname{div}(d_B^n \nabla B^{n+1}) = 0 \quad (39)$$

$$d_B^{n+1} = \frac{\phi'_{1,\epsilon}(|\nabla B^{n+1}|)}{2|\nabla B^{n+1}|} \quad (40)$$

$$\begin{aligned} C_h^{n+1} [\alpha_c + (B^{n+1} - N_h)^2] - \alpha_c \\ - \alpha_c^r \operatorname{div}(d_{C_h}^n \nabla C_h^{n+1}) = 0 \end{aligned} \quad (41)$$

$$d_{C_h}^{n+1} = \frac{\phi'_{2,\epsilon}(|\nabla C_h^{n+1}|)}{2|\nabla C_h^{n+1}|} \quad (42)$$

As we said in the previous section, (40) and (42) give explicitly the values of  $d_B^{n+1}$  and  $d_{C_h}^{n+1}$  while  $B^{n+1}$  and  $C_h^{n+1}$  are solutions of a linear system. Once discretized using finite differences, the linear system can be solved by a Gauss-Seidel method for instance.

We next prove that the discretized algorithm described by (39) to (42) is unconditionally stable.

**Proposition 3.** *Let  $\Omega^d$  correspond to the discretization of  $\Omega$ . Let  $\bar{\mathcal{E}}^d(\Omega)$  be the space of discrete*

functions  $(B, C_1, \dots, C_T)_{i,j}$  such that :

$$m_N \leq B_{i,j} \leq M_N \quad (43)$$

$$0 \leq C_{h,i,j} \leq 1 \quad \text{for } h = 1..T \quad (44)$$

$$0 < m_c \leq \sum_{h=1}^T C_h \leq T \quad (45)$$

$$\text{where } \begin{cases} m_N = \inf_{h=1..T} (i,j) N_{h,i,j} \\ M_N = \sup_{h=1..T} (i,j) N_{h,i,j} \\ m_c = \frac{T \alpha_c}{\alpha_c + (M_N - m_N)^2 + 4} \end{cases} \quad (46)$$

Then, for a given  $(B^n, C_1^n, \dots, C_T^n)$  in  $\bar{\mathcal{E}}^d(\Omega)$ , there exists a unique  $(B^{n+1}, C_1^{n+1}, \dots, C_T^{n+1})$  in  $\bar{\mathcal{E}}^d(\Omega)$  such that (39)-(42) are satisfied.

Remark that the bounds (43) and (44) can be justified if we consider the continuous case (see the proof of the Theorem 2). As for condition (45), it is also very natural if we admit the interpretations of the variables  $C_h$  : if this condition is false, this would mean that the background is never seen at some points which we refuse.

**Proof:** Let us sketch the proof. The first step is to express the discretized equations (39) and (41). Using equations (40) and (42) and the Appendix B for the divergence terms (see the definition of coefficients  $(p_{i+k,j+l})_{(k,l)}$ ), we obtain :

$$B_{i,j}^{n+1} = \sum_{(k,l) \in D} \beta_{k,l}^B B_{i+k,j+l}^{n+1} + \gamma^B \quad (47)$$

$$C_{h,i,j}^{n+1} = \sum_{(k,l) \in D} \beta_{k,l}^{C_h} C_{h,i+k,j+l}^{n+1} + \gamma^{C_h} \quad (48)$$

where :

$$\beta_{k,l}^B = \frac{\alpha_B^r p_{i+k,j+l}(B^n)}{\sum_{h=1}^T C_h^{n2} + \alpha_B^r \sum_{(k,l) \in D} p_{i+k,j+l}(B^n)}$$

$$\gamma^B = \sum_{h=1}^T \frac{N_h C_h^{n2} i_j}{\sum_{h=1}^T C_h^{n2} i_j + \alpha_B^r \sum_{(k,l) \in D} p_{i+k,j+l}(B^n)}$$

$$\beta_{k,l}^{C_h} = \frac{\alpha_C^r p_{i+k,j+l}(C_h^n)}{\alpha_C + (B^n - N_h)_{i,j}^2 + \alpha_C^r \sum_{(k,l) \in D} p_{i+k,j+l}(C_h^n)}$$

$$\gamma_{k,l}^{C_h} = \frac{\alpha_C}{\alpha_C + (B^n - N_h)_{i,j}^2 + \alpha_C^r \sum_{(k,l) \in D} p_{i+k,j+l}(C_h^n)}$$

We then show that we have a contractive application and conclude by applying the fixed point theorem. We refer to [10] for the complete proof which is mainly technical.  $\square$

During this proof we needed to write explicitly the discretized equations to be solved. We give below a sum-up of the precise algorithm. Notice that it is not necessary to compute explicitly the dual variables because they are directly replaced into the divergence operator.

1. /\* **Initializations (may be changed)** \*/
2.  $B^0 \equiv 0, \quad C_h^0 \equiv 1 \quad (\forall h)$
3. /\* **General loop** \*/
4. for(It=0; It ≤ ItNumber; It++) {
5.     /\* \*\*\* **Minimizing in B** \*\*\* \*/
6.     - Compute coefficients  $(p_{i+k,j+l})_{(k,l) \in D}$  corresponding to the divergence discretization for B (see Appendix B)
7.     - Solve the linear system (47) by an iterative method (Gauss-Seidel) to find  $B^{n+1}$
8.     /\* \*\*\* **Minimizing in C<sub>h</sub>** \*\*\* \*/
9.     for(h = 1; h ≤ T; h++) {
10.         - Compute coefficients  $(p_{i+k,j+l})_{(k,l) \in D}$  corresponding to the divergence discretization for  $C_h^n$  (see Appendix B)
11.         - Solve the linear system (48) by an iterative method (Gauss-Seidel) to find  $C_h^{n+1}$
12.     } /\* Loop on h \*/
13. } /\* Loop on It \*/

To conclude this section, we will notice that if  $\alpha_c^r = 0$ , the functions  $(C_h^{n+1})_{h=1..T}$  are in fact obtained explicitly by :

$$C_h^{n+1} = \frac{\alpha_c}{\alpha_c + (B^{n+1} - N_h)^2} \quad (49)$$

As we can imagine, this case permits important reduction of the computational cost since  $T$  linear systems are replaced by  $T$  explicit expressions. We will discuss in Sect. 6 if it is worth regularizing or not the functions  $C_h$ .

## 6. The Numerical Study

This section aims at showing quantitative and qualitative results about this method. Synthetic noisy sequences will be used to estimate rigorously the capabilities of our approach. In all experiments, we will fix the weights of different terms to :  $\alpha_c = 10000, \alpha_b^r = 10$  and we will discuss about the opportunity to choose a non zero coefficient  $\alpha_c^r$ . The purpose of Sect. 6.1 is the quality of the restoration. The Sect. 6.2 is devoted to the motion detection and its sensibility with respect to noise. We will conclude in Sect. 6.3 by real sequences.

### 6.1. About the Restoration

To estimate the quality of the restoration, we used the noisy synthetic sequence presented in Fig. 4 (a)(b). Figure 4 (c) is a representation of the noisy background without the moving objects. We mentioned the value of the Signal to Noise Ratio (SNR) usually used in image restoration to quantify the results quality. We refer to [43] for more details. We recall that the higher the SNR is, the best the quality is. Classically used to extract the foreground from the background, the median (see Fig. 4 (d)) appears to be inefficient. The average in time of the sequence (see Fig 4 (e)), although it permits a noise reduction, keeps the trace of the moving objects. The Fig. 4 (f) is the result that we obtained.

To conclude that section, let us mention that we also tried the case  $\alpha_c^r = 0$ , that is to say we do not regularized the functions  $C_h$ . The resulting SNR was 14, to be compared with 14.4 ( $\alpha_c^r \neq 0$ ). This kind of results has been observed in all ex-

periments : regularizing the functions  $C_h$  does not seem to influence the quality of the restored background. Naturally if we are just interested to the movement detection, this regularization may be important. However, this point has to be better investigated and more experimental results have to be considered before to conclude.

### 6.2. The Sensitivity of Motion Detection With Respect to Noise

In this section, we aim at showing the robustness of our method with respect to noise. To this end, we choose a synthetic sequence (see Fig. 5) where a grey circle is translating from left to right in front of a textured background.

To estimate the sensitivity of the algorithm, we corrupted the sequence by gaussian noise of different variance (from 5 to 50). We give in Fig. 1 the value of the SNR of the corrupted sequences for each variance.

Figure 7 presents five typical results obtained for different values of  $\sigma$  ( $\sigma=5,15,25,35,45$ ). The second one gives qualitative informations concerning the quality of the restoration and the motion detection. The criterion used to decide whether a pixel belongs to the background or not is : if  $C_h(i,j) > \text{threshold}$ , then the pixel  $(i,j)$  of the image number  $h$  belongs to the background. Otherwise, it belongs to a moving object. The threshold has been fixed to 0.25 in all experiments.

We can observe that when the SNR of the data is more than 8 (corresponding to  $\sigma \approx 25$ ), results are particularly precise : The SNR of the background is more than 20 (see Fig. 2) and the error detections are less than 5 percent (see Fig. 3). When the SNR of the data is less than 8, the motion detection errors grow rapidly but the quality of the restored background still remains correct. See for instance the last row of Fig. 7 obtained for  $\sigma = 45$  : the triangles on both sides are well recovered (observe the strong noise in the sequence).

Finally, notice that same parameters ( $\alpha_b^r, \alpha_c, \alpha_c^r$ ) have been used for all experiments. Generally speaking, we remarked that the algorithm performs well on a wide variety of sequences with the same set of parameters ( $\alpha_b^r, \alpha_c, \alpha_c^r$ ) = (10,  $10^5, 10^3$ ).



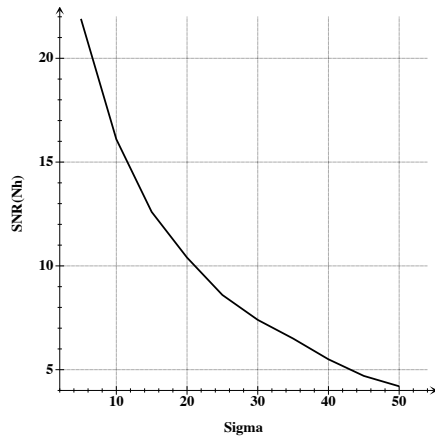


Fig. 1. Signal to Noise Ratio of the data as a function of the variance.

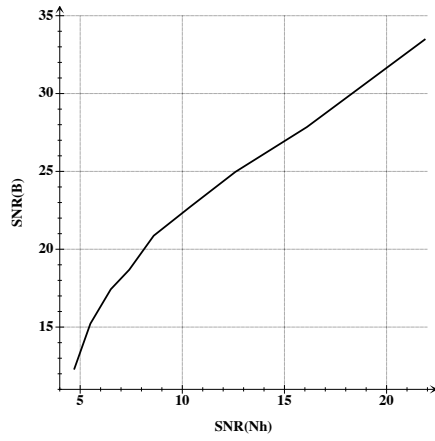


Fig. 2. SNR of the background as a function of the SNR of the data.

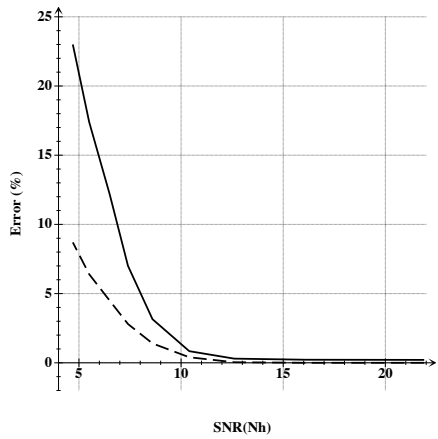


Fig. 3. dotted (resp. plain) line : percentage of bad detections for the moving regions (resp. static background) as a function of the SNR of the data.

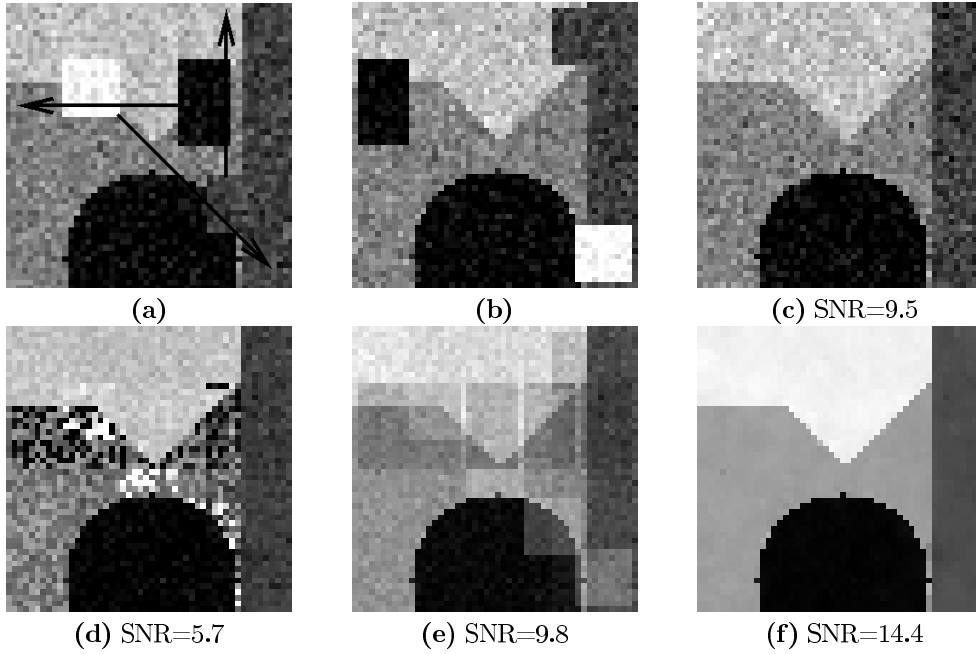


Fig. 4. Results on a synthetic sequence (5 images) (a) Description of the sequence (first image) (b) Last image of the sequence (c) The noisy background without any objects (d) Mediane (e) Average (f) Restored background ( $\alpha_c^r \neq 0$ )

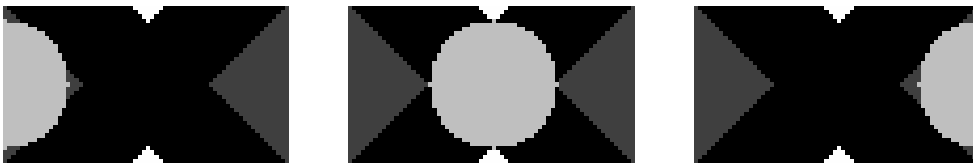


Fig. 5. Three images of the initial synthetic sequence (35 images are available)

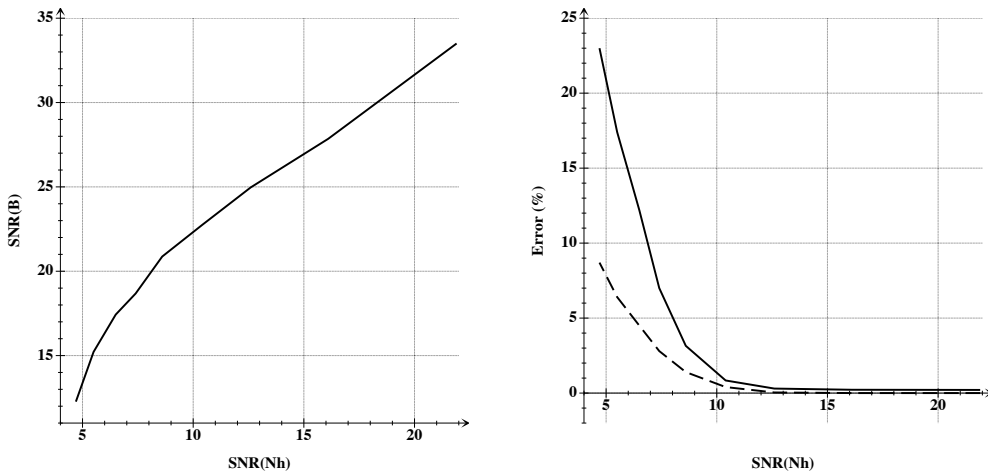
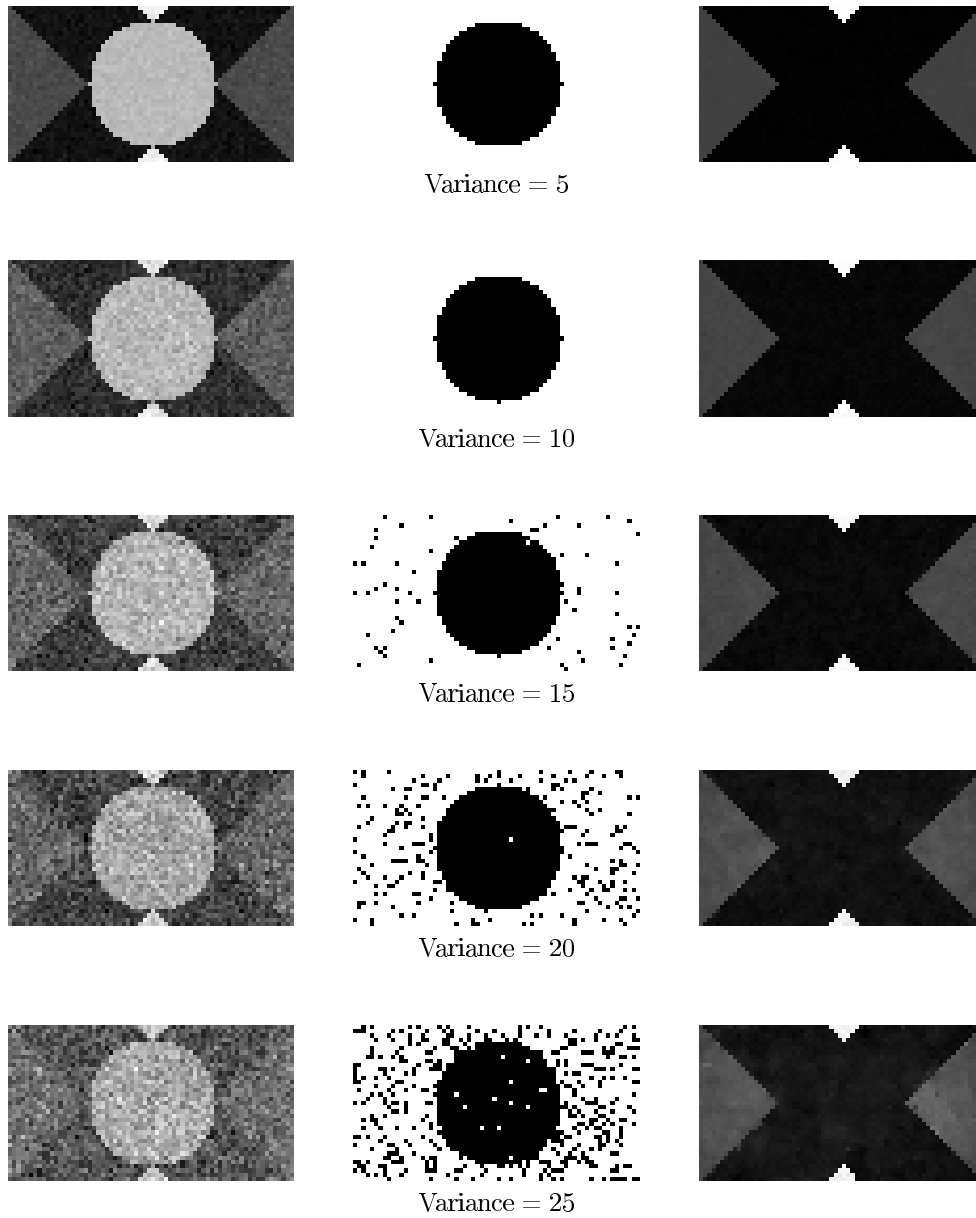


Fig. 6. **Left** : SNR of the background as a function of the SNR of the data. **Right** : *dotted* (resp. *plain*) line : percentage of bad detections for the moving regions (resp. static background) as a function of the SNR of the data.



*Fig. 7.* **Left :** One image of the noisy sequence. **Middle :** The motion detection based on variable  $C_h$  at the same time. **Right :** The restored background  $B$ . **From top to bottom :** Results for different variances of the gaussian noise (5,15,25,35,45).

### 6.3. Results on Real Sequences

Numerous real sequences have been tested using this methodology. We will present some results where the background of the scene is seen most of the time. To be more precise, we mention that some experiments have been done where some people were hiding the background more than sixty percent of the time. In that case, the background found does not correspond to the real static regions and takes into account some people for the reconstruction. One possible way to avoid this could be to add some a priori information of the movement.

The first real sequence is presented in Fig. 8 (a)-(b). A small noise is introduced by the camera and certainly by the hard weather conditions. Notice the reflections on the ground which is frozen. We show in Fig. 8 (c) the average in time of the sequence. The restored background is shown in Fig. 8 (d). As we can see, it has been very well found and enhanced. Figure 8 (e) is a representation of the function  $C_h$  (using a threshold of 0.5) and we show in Fig 8 (f) the associated dual variable  $d_{C_h}$ .

The second sequence is more noisy than the first one. Its description is given in Fig. 9 (a). To evaluate the quality of the restoration, we show a close-up of the same region for one original image (see Fig. 9 (b)), the average in time (see Fig. 9 (c)) and the restored background  $B$  (see Fig. 9 (d)). The detection of moving regions is displayed in Fig. 9 (e). Notice that some sparse motion have been detected at the right bottom and at the left side of the two persons. They correspond to the motion of a bush and the shadow of a tree due to the wind.

The last sequence is taken from an highway (see Fig. 10). We give two images (Fig. 10 (a) and (b)) and the corresponding motion detection below (Fig. 10 (c) and (d)). Finally, we show in Fig. 10 (e) the restored background. Notice that there is a black zone at the top of the road which comes from the fact that there are always cars in that region.

Notice that corresponding animations are available in the Pierre Kornprobst's home page <sup>4</sup>.

## 7. Conclusion

We have presented in this article an original coupled method for the problem of image sequence restoration and motion segmentation. A theoretical study in the space of bounded variations showed us that the problem was well-posed. We then proposed a convergent stable algorithm to approximate the unique solution of the initial minimization problem.

This original way to restore image sequence has been proved to give very promising result. A straightforward extension to color image sequences has recently been developed. To complete this work, several ideas are considered : use the motion segmentation part to restore also the moving regions, think about possible extensions for non-static cameras. This is the object of our current work.

### Appendix A

#### The Half Quadratic Minimization Theorem

This theorem has been inspired by Geman and Reynolds [30] and proposed by Aubert [8].

**Theorem 3.** *Let  $\varphi : [0, +\infty[ \rightarrow [0, +\infty[$  be such that:*

$$\varphi(\sqrt{t}) \text{ is concave on } ]0, +\infty[. \quad (1)$$

*Let  $L$  and  $M$  be defined as:  $L = \lim_{t \rightarrow +\infty} \frac{\phi'(t)}{2t}$  and  $M = \lim_{t \rightarrow 0^+} \frac{\phi'(t)}{2t}$ . Then, there exists a convex and decreasing function  $\psi : ]L, M] \rightarrow [\beta_1, \beta_2]$  such that*

$$\varphi(t) = \inf_{L \leq d \leq M} (dt^2 + \psi(d)) \quad (2)$$

*where:  $\beta_2 = \lim_{t \rightarrow +\infty} \left( \phi(t) - t^2 \frac{\phi'(t)}{2t} \right)$  and  $\beta_1 = \lim_{t \rightarrow 0^+} \phi(t)$  Moreover, for every fixed  $t \geq 0$  the value  $d_t$  for which the minimum is reached is unique and given by:*

$$d_t = \frac{\phi'(t)}{2t} \quad (3)$$

In addition, we can give the expression of the function  $\Psi$  with respect to  $\phi$ . If we note  $\theta(t) =$

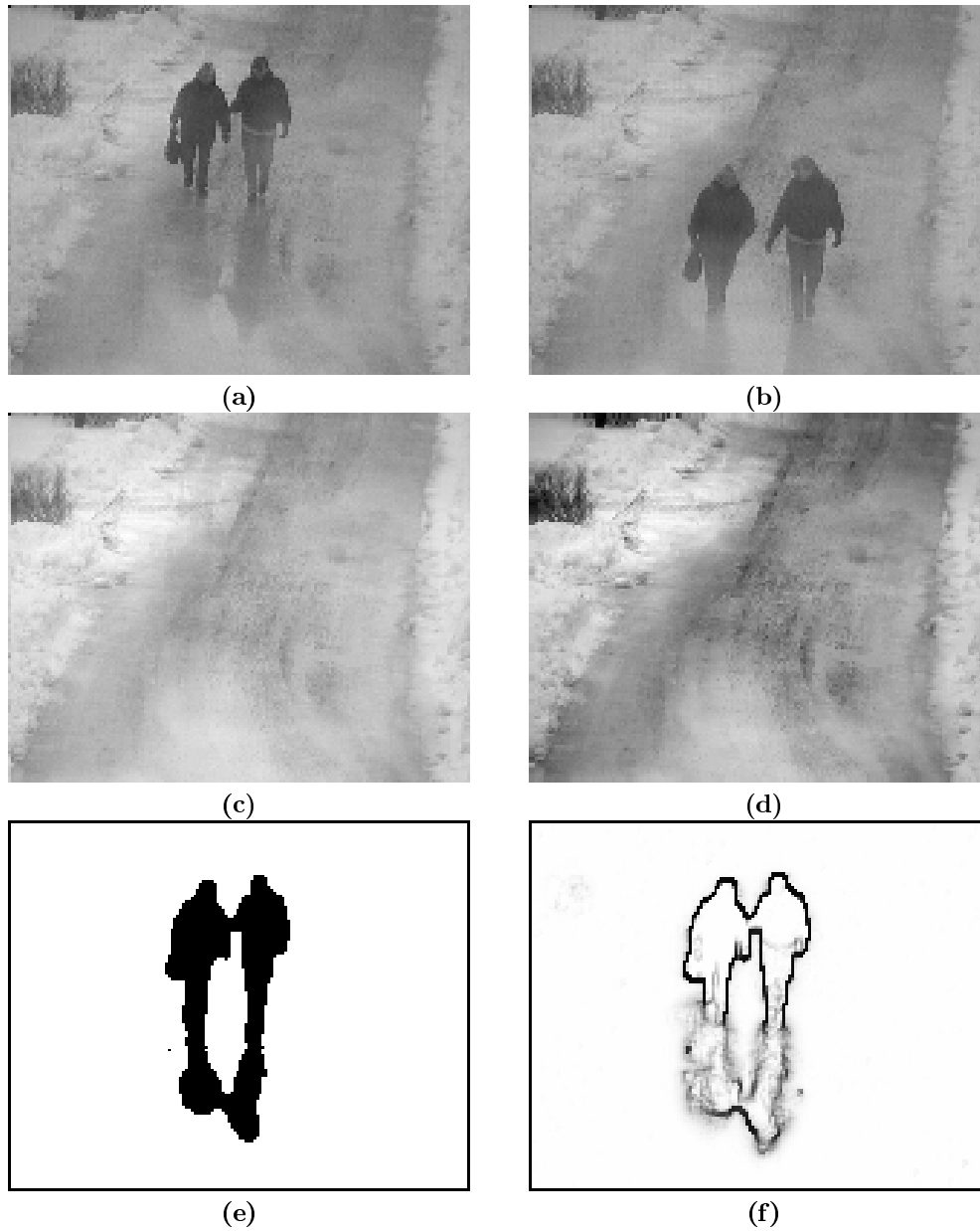


*Fig. 8.* Sweden Sequence : (a) and (b) Description of the sequence (55 images available). Two people are walking from top to bottom. This sequence is available from the web site <http://www.iem.it/is/is.html>. (c) The average over the time. (d) The restored background  $B$ . (e) Function  $C_h$  associated to the image (a) (a threshold of 0.5 has been used). (f) The dual variable  $d_{C_h}$  associated to the image (a).

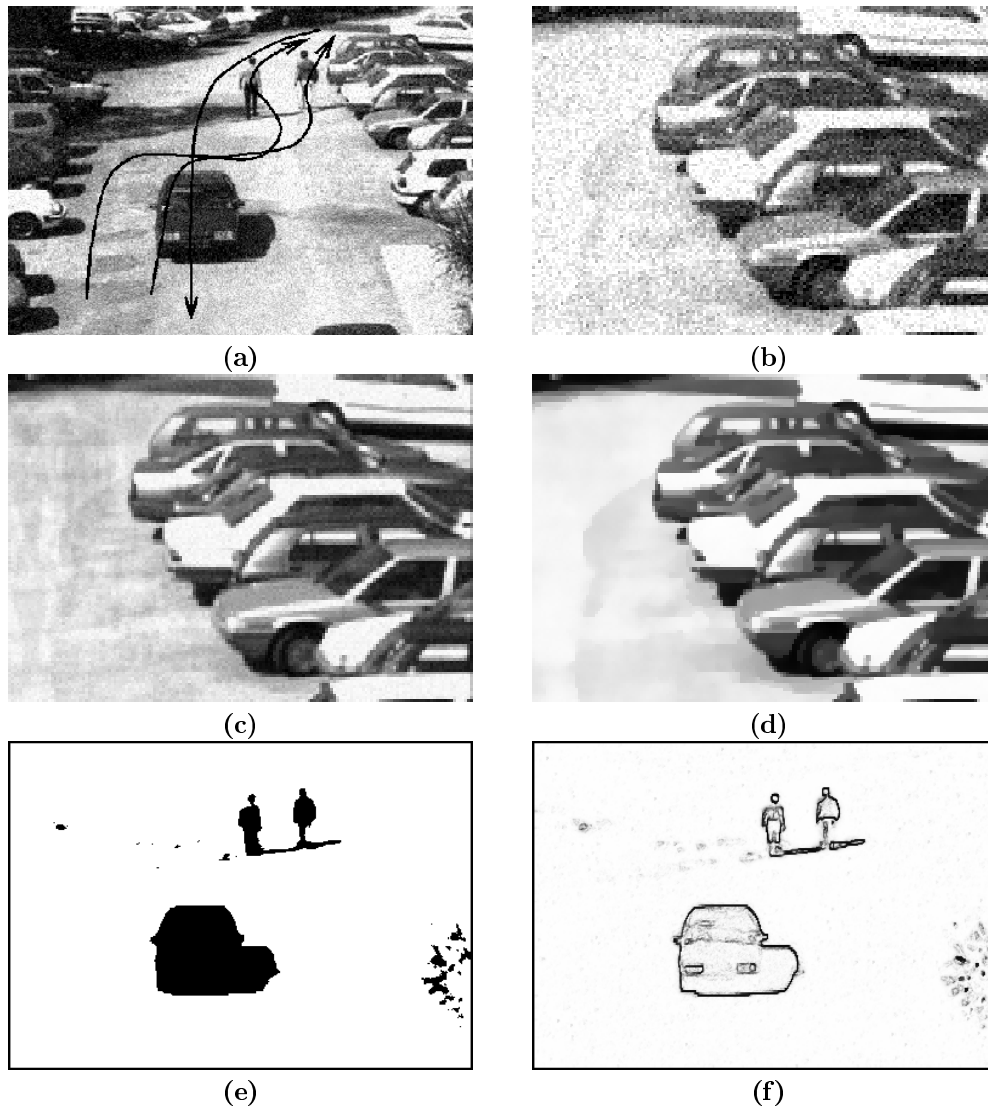


*Fig. 9.* INRIA Sequence : (a) Description of the sequence (12 images available). (b) Zoom on a upper right part of the original sequence (without objects). (c) Zoom on the mean image. (d) Zoom on the restored background  $B$ . (e) The function  $C_h$  thresholded. (f) The dual variable  $d_{C_h}$ .

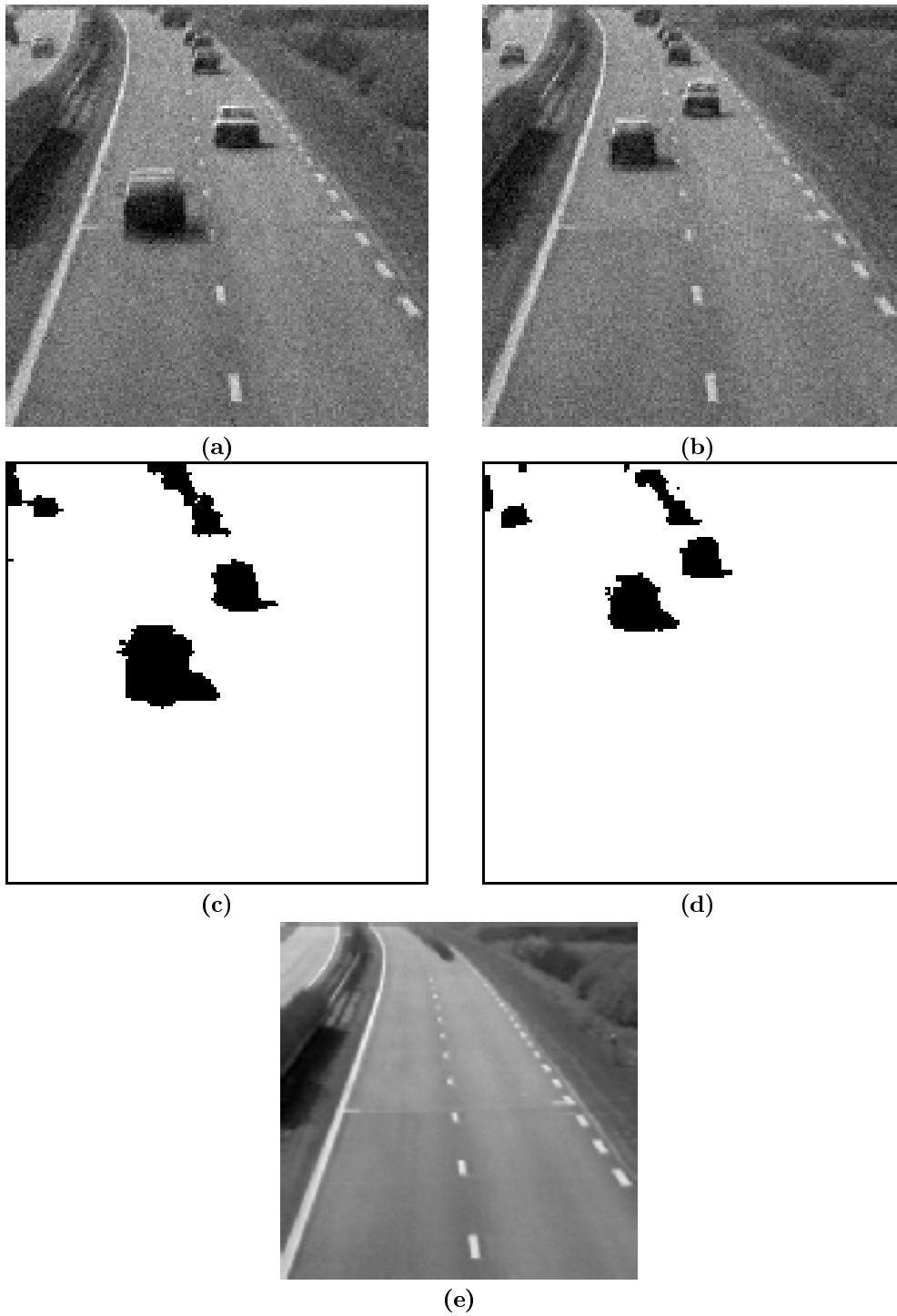


*Fig. 10.* Highway Sequence : (a) and (b) Two images from the sequence (90 images available). (c) and (d) Corresponding  $C_h$  functions. (e) The restored background.

$\phi(\sqrt{t})$ , then :

$$\Psi(t) = \theta((\theta')^{-1}(t)) - t(\theta')^{-1}(t)$$

However, notice that this expression will never be used explicitly.

## Appendix B

### On Discretizing the Divergence Operator

Let  $d$  and  $A$  given at nodes  $(i, j)$ . The problem is to get an approximation of  $\text{div}(d\nabla A)$  at the node  $(i, j)$ . We denote by  $\delta^{x_1}$  and  $\delta^{x_2}$  the finite difference operators defined by :

$$\delta^{x_1} A_{i,j} = A_{i+\frac{1}{2},j} - A_{i-\frac{1}{2},j}$$

$$\delta^{x_2} A_{i,j} = A_{i,j+\frac{1}{2}} - A_{i,j-\frac{1}{2}}$$

Using that notation, Perona and Malik [58] proposed the following approximation :

$$\begin{aligned} \text{div}(d\nabla A)_{i,j} &= \frac{\partial}{\partial x_1} \left( d \frac{\partial A}{\partial x_1} \right) + \frac{\partial}{\partial x_2} \left( d \frac{\partial A}{\partial x_2} \right) \\ &\approx \delta^{x_1} (d \delta^{x_1} A_{i,j}) + \delta^{x_2} (d \delta^{x_2} A_{i,j}) \\ &\approx \begin{pmatrix} 0 & d_{i,j+\frac{1}{2}} & 0 \\ d_{i-\frac{1}{2},j} & -S^P & d_{i+\frac{1}{2},j} \\ 0 & d_{i,j-\frac{1}{2}} & 0 \end{pmatrix} \star A_{i,j} \end{aligned} \quad (1)$$

where the symbol  $\star$  denotes the convolution and  $S^P$  is the sum of the four weights in the principal directions. Notice that we need to estimate the function  $d$  at intermediate nodes. Our aim is to extend this approximation so that we could take into account the values of  $A$  at the diagonal nodes :

$$\begin{aligned} \text{div}(d\nabla A)_{i,j} &= \alpha_P \begin{pmatrix} 0 & d_{i,j+\frac{1}{2}} & 0 \\ d_{i-\frac{1}{2},j} & -S^P & d_{i+\frac{1}{2},j} \\ 0 & d_{i,j-\frac{1}{2}} & 0 \end{pmatrix} \star A_{i,j} \\ &+ \alpha_D \begin{pmatrix} d_{i-\frac{1}{2},j+\frac{1}{2}} & 0 & d_{i+\frac{1}{2},j+\frac{1}{2}} \\ 0 & -S^D & 0 \\ d_{i-\frac{1}{2},j-\frac{1}{2}} & 0 & d_{i+\frac{1}{2},j-\frac{1}{2}} \end{pmatrix} \star A_{i,j} \end{aligned} \quad (2)$$

where  $\alpha_P$  and  $\alpha_D$  are two weights to be discussed, and  $S^D$  is the sum of the four weights in the diagonal directions. Approximation (2) is consistent if and only if :

$$\alpha_P + 2\alpha_D = 1 \quad (3)$$

Now, there remains one degree of freedom. Two possibilities have been considered :

$$(\alpha_P, \alpha_D) = \left( \frac{1}{2}, \frac{1}{4} \right) \quad (4)$$

$$(\alpha_P, \alpha_D) = \text{functions of } d \text{ (See Fig. 10)} \quad (5)$$

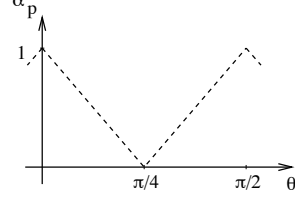


Fig. B.1.  $\alpha_P = \alpha_P(\theta)$  is a  $\pi/2$  periodic function where  $\theta$  is the direction of the gradient of  $d$ . Notice that  $\alpha_D$  can be deduced from the consistency condition is then computed thanks to the consistency condition.

Before going further, remark that any kind of discretization leads to :

$$\begin{aligned} \text{div} \left( \frac{\phi'(|\nabla A|)}{|\nabla A|} \nabla A \right)_{i,j} &\approx \\ &\sum_{(k,l) \in D} p_{i+k,j+l}(A) A_{i,j} - \left( \sum_{(k,l) \in D} p_{i+k,j+l}(A) \right) A_{i,j} \end{aligned} \quad (6)$$

where  $D = \{(k, l) \neq (0, 0) \in [-1, 0, 1]^2\}$  and  $(p_{i+k,j+l})_{(k,l) \in D}$  verifying :

$$0 \leq p_{i+k,j+l} \leq 1 \quad \text{and} \quad \sum_{(k,l) \in D} p_{i+k,j+l} \leq 4 \quad (7)$$

To compare these different discretizations, we made numerical experiments with the image restoration problem where such kind of operator have to be discretized. We recall that for a given  $d_I^n$ , we need to find  $I^{n+1}$  such that :

$$I^{n+1} - N - \alpha^r \text{div}(d_I^n \nabla I^{n+1}) = 0$$

We refer to section 2 for more details. The value of  $d_I^n$  ( $= \frac{\phi'(|\nabla I^n|)}{2|\nabla I^n|}$ ) at intermediate nodes is computed by interpolation (see [58]).

We tested these different discretizations on a noisy test image using quantitative measures. We checked that (2) permits to restore identically edges in principal or diagonal directions. Moreover, we observed that choosing  $\alpha_P$  adaptatively (5) gave more precise results than (4). We used this approximation (5) in our experiments.



## Appendix C

### Proof of Lemma 1

**Proof:** Let us first recall the Lebesgue decomposition of the measure  $\phi(Du)$  :

$$\int_{\Omega} \phi(Du) = \underbrace{\int_{\Omega} \phi(|\nabla u|) dx}_{\text{term 1}} + \underbrace{\int_{S_u} |u^+ - u^-| \mathcal{H}^{N-1}}_{\text{term 2}} + \underbrace{\int_{\Omega/S_u} |C_u|}_{\text{term 3}}$$

We are going to show that cutting the function  $u$  using the function  $\varphi_{\alpha,\beta}$  permits to reduce each term. To simplify notations, we will sometimes use the notation  $\hat{u}$  for the truncated function  $\varphi_{\alpha,\beta}(u)$

**Term 1:** let  $\Omega_c = \{x \in \Omega / u(x) \leq \alpha \text{ or } u(x) \geq \beta\}$  and  $\Omega_i = \Omega / \Omega_c$ . Thanks to [37], we have  $\int_{\Omega_i} \phi(|\nabla \hat{u}|) dx = \int_{\Omega_i} \phi(|\nabla u|) dx$ . Consequently :

$$\begin{aligned} \int_{\Omega} \phi(|\nabla \hat{u}|) dx &= \int_{\Omega_i} \phi(|\nabla u|) dx + \int_{\Omega_c} \phi(|\nabla \hat{u}|) dx \\ &\leq \int_{\Omega} \phi(|\nabla u|) dx \end{aligned} \quad (1)$$

**Term 2:** using results proved in [5], we know that :

$$\begin{aligned} S_{\hat{u}} &\subset S_u \\ \hat{u}^+ &= \varphi_{\alpha,\beta}(u^+) \text{ and } \hat{u}^- = \varphi_{\alpha,\beta}(u^-) \end{aligned}$$

Thanks to these results, and since  $\varphi_{\alpha,\beta}$  is Lipschitz continuous with a constant equals to 1, we have :

$$\begin{aligned} \int_{S_{\hat{u}}} |\hat{u}^+ - \hat{u}^-| \mathcal{H}^{N-1} &\leq \int_{S_u} |u^+ - u^-| \mathcal{H}^{N-1} \\ &\leq \int_{S_u} |u^+ - u^-| \mathcal{H}^{N-1} \end{aligned} \quad (2)$$

**Term 3:** we need to understand how is the Cantor part of the distributional derivative of the composed function  $\varphi_{\alpha,\beta}(u)$ . Vol'pert [70] first proposed a chain rule formula for functions  $v = \varphi(u)$  for  $u \in BV(\Omega)$  and when  $\varphi$  is continuously differentiable. Ambrosio and Dal Maso [6] gave extended results for functions  $\varphi$  uniformly Lipschitz continuous. Since  $u$  is scalar, it is demonstrated in [6] that we can write :

$$C(\varphi_{\alpha,\beta}(u)) = \varphi'_{\alpha,\beta}(\tilde{u}) C(u) \quad |Du|\text{-a.e. on } \Omega/S_u \quad (3)$$

where  $\tilde{u}$  is the approximate limit of  $u$  defined by :

$$\lim_{r \rightarrow 0^+} r^{-N} \int_{B(x,r)} |u(y) - \tilde{u}(x)| dy = 0$$

where  $B(x,r)$  is the closed ball with center  $x$  and radius  $r$ . Moreover, we have :

$$\int_{\Omega/S_{\hat{u}}} |C_{\hat{u}}| = \int_{\Omega/S_u} |C_u| + \underbrace{\int_{S_u/S_{\hat{u}}} |C_{\hat{u}}|}_{(\equiv 0)} \quad (4)$$

Notice that the second integral equals to zero because the Hausdorff dimension of the set  $S_u/S_{\hat{u}}$  is at most  $N-1$  and we know that for any  $v \in BV(\Omega)$  and any set  $S$  of Hausdorff dimension at most  $N-1$ , we have  $C_v(S) = 0$ . Then, using the chain rule formula (3), we have :

$$\int_{\Omega/S_{\hat{u}}} |C_{\hat{u}}| \leq \|\varphi'_{\alpha,\beta}\|_{L^\infty} \int_{\Omega/S_u} |C_u| \leq \int_{\Omega/S_u} |C_u| \quad (5)$$

Finally, using results (1), (2), (5) permits to write :

$$\int_{\Omega} \phi(D\varphi_{\alpha,\beta}(u)) \leq \int_{\Omega} \phi(Du)$$

This concludes the proof.  $\square$

## Notes

1. <http://www.ina.fr/INA/Recherche/Aurora/index.en.html>
2. <http://www.spd.eee.strath.ac.uk/users/harve/noblesse.html>
3. <http://www.esat.kuleuven.ac.be/~koniijn/improofs.html>
4. <http://www.inria.fr/robotvis/personnel/pkornp/pkornp-eng.html>

## References

1. T. Aach and A. Kaup. Bayesian algorithms for adaptive change detection in image sequences using markov random fields. *Signal Processing: Image Communication*, 7:147–160, 1995.
2. R. Acart and C.R. Vogel. Analysis of bounded variation penalty methods for ill-posed problems. *Inverse Problems*, 10:1217–1229, 1994.
3. L. Alvarez, P-L. Lions, and J-M. Morel. Image selective smoothing and edge detection by nonlinear diffusion (ii). *SIAM Journal of numerical analysis*, 29:845–866, 1992.
4. Luis Alvarez and Luis Mazorra. Signal and image restoration using shock filters and anisotropic diffusion. *SIAM Journal of numerical analysis*, 31(2):590–605, April 1994.
5. L. Ambrosio. A compactness theorem for a new class of functions of bounded variation. *Boll. Unione Mat. Ital.*, VII(4):857–881, 1989.
6. L. Ambrosio and G. Dal Maso. A general chain rule for distributional derivatives. *Proc. Am. Math. Soc.*, 108(3):691–702, 1990.
7. G. Anzellotti. The euler equation for functionals with linear growth. *Trans. Am. Math. Soc.*, 290(2):483–501, August 1985.
8. G. Aubert, M. Barlaud, L. Blanc-Feraud, and P. Charbonnier. Deterministic edge-preserving regularization in computed imaging. *IEEE Trans. Imag. Process.*, 5(12), February 1997.
9. G. Aubert, R. Deriche, and P. Kornprobst. A mathematical study of the regularized optical flow problem in the space  $BV(\Omega)$ . Technical Report 503, Université de Nice-Sophia Antipolis, December 1997.
10. G. Aubert, R. Deriche, and P. Kornprobst. A variational method and its mathematical study in image sequence analysis. Technical Report 3415, INRIA, April 1998.
11. G. Aubert and L. Vese. A variational method in image recovery. *SIAM J. Numer. Anal.*, 34(5):1948–1979, October 1997.
12. M.J. Black, G. Sapiro, D.H. Marimont, and D. Heeger. Robust anisotropic diffusion. *IEEE Trans. Imag. Proc.*, 7(3):421–432, 1998. Special Issue on Partial Differential Equations and Geometry-Driven Diffusion in Image Processing and Analysis.
13. Andrew Blake and Andrew Zisserman. *Visual Reconstruction*. MIT Press, 1987.
14. P. Blomgren and T.F. Chan. Color tv: Total variation methods for restoration of vector-valued images. *IEEE Trans. Imag. Proc.*, 7(3):304–309, 1998. Special Issue on Partial Differential Equations and Geometry-Driven Diffusion in Image Processing and Analysis.
15. G. Bouchitté, I. Fonseca, and L. Mascarenhas. A global method for relaxation. Technical report, Université de Toulon et du Var, May 1997.
16. J. Boyce. Noise reduction of image sequences using adaptative motion compensated frame averaging. In *IEEE ICASSP*, volume 3, pages 461–464, 1992.
17. J.C. Brailean and A.K. Katsaggelos. Simultaneous recursive displacement estimation and restoration of noisy-blurred image sequences. *IEEE Transactions on Image Processing*, 4(9):1236–1251, September 1995.
18. H. Brezis. *Opérateurs maximaux monotones et semi-groupes de contractions dans les espaces de Hilbert*. North-Holland Publishing Comp, Amsterdam-London, 1973.
19. O. Buisson, B. Besserer, S. Boukir, and F. Helt. Deterioration detection for digital film restoration. In *Computer Vision and Pattern Recognition*, pages 78–84, Puerto Rico, June 1997.
20. V. Caselles, J.M. Morel, G. Sapiro, and A. Tannenbaum. Introduction to the special issue on partial differential equations and geometry-driven diffusion in image processing and analysis. *IEEE Transactions on Image Processing*, 7(3):269–273, 1998.
21. A. Chambolle and P-L. Lions. Image recovery via total variation minimization and related problems. *Numer. Math.*, 76(2):167–188, 1997.
22. I. Cohen. Nonlinear variational method for optical flow computation. In *Proceedings 8th SCIA*, volume 1, pages 523–530, 1993.
23. Laurent D. Cohen. Auxiliary variables and two-step iterative algorithms in computer vision problems. *ICCV*, 1995.
24. G.-H. Cottet and L. Germain. Image processing through reaction combined with nonlinear diffusion. *Mathematics of Computation*, 61(204):659–673, October 1993.
25. F. Demengel and R. Temam. Convex functions of a measure and applications. *Indiana University Mathematics Journal*, 33:673–709, 1984.
26. R. Deriche and O. Faugeras. Les EDP en traitement des images et vision par ordinateur. Technical report, INRIA, November 1995. A more complete version of this Research Report has appeared in the French Revue "Traitement du Signal". Volume 13 - No 6 - Special 1996.
27. E. Dubois and S. Sabri. Noise reduction in image sequences using motion-compensated temporal filtering. *IEEE Transactions on Communications*, 32(7):826–831, July 1984.
28. L. C. Evans and R. F. Gariepy. *Measure Theory and Fine Properties of Functions*. CRC, 1992.
29. H. Federer. *Geometric Measure Theory*. Classics in Mathematics. Springer-Verlag, Berlin . Heidelberg . New York, 1969.
30. D. Geman and G. Reynolds. Constrained restoration and the recovery of discontinuities. *IEEE Transactions on Pattern Analysis and Machine Intelligence*, 14(3):367–383, 1993.
31. Stuart Geman, Donald E McClure, and Donald Geman. A nonlinear filter for film restoration and other problems in image processing. *CVGIP : Graphical Models and Image Processing*, 54(4):281–289, July 1992.
32. E. De Giorgi and T. Franzoni. Su un tipo di convergenza variazionale. *Atti Accad. Naz. Lincei Rend. Cl. Sci. Fis. Mat. Natur.*, 68:842–850, 1975.
33. E. Giusti. *Minimal Surfaces and Functions of Bounded Variation*. Birkhäuser, 1984.
34. C. Goffman and J. Serrin. Sublinear functions of measures and variational integrals. *Duke Math J.*, 31:159–178, 1964.
35. F. Guichard. *Axiomatisation des analyses multi-échelles d'images et de films*. PhD thesis, Université Paris IX Dauphine, 1994.

36. K. Karmann, A. Brandt, and R. Gerl. Moving object segmentation based on adaptive reference images. *Signal Processing: Theories and Applications*, V:951–954, 1990.
37. D. Kinderlehrer and G. Stampacchia. *An Introduction to Variational Inequalities and Their Applications*. Academic Press, 1980.
38. A. Kokaram. Reconstruction of severely degraded image sequences. In *International Conference on Image Applications and Processing*, Florence, Italy, 1997.
39. A. C. Kokaram and S.J. Godsill. A system for reconstruction of missing data in image sequences using sampled 3d ar models and mrf motion priors. In Bernard Buxton, editor, *Proceedings of the 4th European Conference on Computer Vision*, pages 613–624, Cambridge, UK, April 1996.
40. P. Kornprobst. *Contributions à la restauration d'images et à l'analyse de séquences : Approches Variationnelles et Equations aux Dérivées Partielles*. PhD thesis, Université de Nice-Sophia Antipolis, 1998.
41. P. Kornprobst, R. Deriche, and G. Aubert. Image restoration via PDE's. In *First Annual Symposium on Enabling Technologies for Law Enforcement and Security - SPIE Conference 2942 : Investigative Image Processing.*, Boston, Massachusetts, USA., November 1996.
42. P. Kornprobst, R. Deriche, and G. Aubert. Image coupling, restoration and enhancement via PDE's. In *International Conference on Image Processing*, volume II of III, pages 458–461, Santa-Barbara, California, October 1997.
43. P. Kornprobst, R. Deriche, and G. Aubert. Nonlinear operators in image restoration. In *Proceedings of the International Conference on Computer Vision and Pattern Recognition*, pages 325–331, Puerto-Rico, June 1997. IEEE.
44. P. Kornprobst, R. Deriche, and G. Aubert. Edp, débruitage et réhaussement en traitement d'image: Analyse et contributions. In *11 ème Congres RFIA*. AFCET, January 1998.
45. S. Liou and R. Jain. Motion detection in spatio-temporal space. *Computer Vision, Graphics and Image Understanding*, (45):227–250, 1989.
46. R. Malladi and J.A. Sethian. Image processing: Flows under min/max curvature and mean curvature. *Graphical Models and Image Processing*, 58(2):127–141, March 1996.
47. G. Dal Maso. *An introduction to  $\Gamma$ -convergence*. Progress in Nonlinear Differential Equations and their Applications. Birkhauser, 1993.
48. N.G. Meyers. An  $L^p$ -estimate for the gradient of solutions of second order elliptic divergence equations. *Ann. Scuola Norm. Sup. Pisa*, III(17):189–206, 1963.
49. N.G. Meyers and A. Elcrat. Some results on regularity for solutions of non-linear elliptic systems and quasi-regular functions. *Duke math. J.*, 42:121–136, 1975.
50. L. Moisan. *Traitement numérique d'images et de films : équations aux dérivées partielles préservant forme et relief*. PhD thesis, Université Paris IX Dauphine, June 1997.
51. J-M. Morel and S. Solimini. Segmentation of images by variational methods: A constructive approach. *Rev. Math. Univ. Complut. Madrid*, 1:169–182, 1988.
52. R.D. Morris. *Image Sequence Restoration using Gibbs Distributions*. PhD thesis, Cambridge University, England, 1995.
53. D. Mumford and J. Shah. Optimal approximations by piecewise smooth functions and associated variational problems. *Comm. Pure Appl. Math.*, 42:577–684, 1989.
54. N. Nordström. Biased anisotropic diffusion - a unified regularization and diffusion approach to edge detection. *Image and Vision Computing*, 8(11):318–327, 1990.
55. N. Paragios and R. Deriche. A PDE-based Level Set Approach for Detection and Tracking of Moving Objects. In *Proceedings of the 6th International Conference on Computer Vision*, Bombay, India, January 1998. IEEE Computer Society Press.
56. N. Paragios and G. Tziritas. Detection and localization of moving objects in image sequences. *FORTH-Hellas Technical Report, Accepted for publication in Signal Processing: Image Communication*, October 1996.
57. Nikolaos Paragios and Rachid Deriche. Detecting multiple moving targets using deformable contours. In *International Conference on Image Processing*, volume II of III, pages 183–186, Santa-Barbara, California, October 1997.
58. P. Perona and J. Malik. Scale-space and edge detection using anisotropic diffusion. *IEEE Transactions on Pattern Analysis and Machine Intelligence*, 12(7):629–639, July 1990.
59. M. Proesmans, E. Pauwels, and L. Van Gool. *Coupled Geometry-Driven Diffusion Equations for Low-Level Vision*, pages 191–228. Computational imaging and vision. Kluwer Academic Publishers, 1994.
60. L. Rudin and S. Osher. Total variation based image restoration with free local constraints. In *International Conference on Image Processing*, volume I, pages 31–35, November 1994.
61. G. Sapiro and V. Caselles. Contrast enhancement via image evolution flows. *Graphical Models and Image Processing*, 59(6):407–416, 1997.
62. G. Sapiro and D.L. Ringach. Anisotropic diffusion of multivalued images with applications to color filtering. *IEEE Transactions on Image Processing*, 5(11):1582–1585, 1996.
63. G. Sapiro, A. Tannenbaum, Y.L. You, and M. Kaveh. Experiments on geometric image enhancement. In *International Conference on Image Processing*, 1994.
64. C. Schnörr. Unique reconstruction of piecewise-smooth images by minimizing strictly convex non-quadratic functionals. *Journal of Mathematical Imaging and Vision*, 4:189–198, 1994.
65. Jayant Shah. A common framework for curve evolution, segmentation and anisotropic diffusion. *IEEE*, 1996.
66. R.L. Stevenson, B.E. Schmitz, and E.J. Delp. Discontinuity preserving regularization of inverse visual problems. *IEEE Transactions on Systems, Man, and Cybernetics*, 24(3):455–469, March 1994.
67. D.M. Strong and T.F. Chan. Spatially and scale adaptive total variation based regularization and anisotropic diffusion in image processing. Technical Report 46, UCLA, November 1996.

68. A.N. Tikhonov and V.Y. Arsenin. *Solutions of Ill-posed Problems*. Winston and Sons, Washington, D.C., 1977.
69. L. Vese. *Problèmes variationnels et EDP pour l'analyse d'images et l'évolution de courbes*. PhD thesis, Université de Nice Sophia-Antipolis, November 1996.
70. A.I. Vol'pert. The spaces BV and quasilinear equations. *Math. USSR-Sbornik*, 2(2):225–267, 1967.
71. J. Weickert. *Anisotropic Diffusion in Image Processing*. PhD thesis, University of Kaiserslautern, Germany, Laboratory of Technomathematics, January 1996.
72. J. Weickert. *Anisotropic Diffusion in Image Processing*. Teubner-Verlag, Stuttgart, 1998.
73. O. Wenstop. Motion detection from image information. *Proceedings in Scandinavian Conference on Image Analysis*, pages 381–386, 1983.
74. Y.L. You, M. Kaveh, W.Y. Xu, and A. Tannenbaum. Analysis and Design of Anisotropic Diffusion for Image Processing. In *International Conference on Image Processing*, volume II, pages 497–501, November 1994.
75. W.P. Ziemer. *Weakly Differentiable Functions*. Springer-Verlag, 1989.

**Pierre Kornprobst** received the Thèse d'Etat es-science Mathématiques from the University of Nice in november 1998. His research interests include viscosity solution, nonlinear parabolic equations, optimization problems and calculus of variations. He is interested in the application of these notions to Computer Vision topics like image restoration and enhancement, optical flow computation, image sequence analysis (restoration and segmentation), medical imagery, etc. To find out more about his research and some selected publications take a look at

<http://www.inria.fr/robotvis/personnel/pkornp/pkornp-eng.html>

**Rachid Deriche** obtained the Ph.D degree from the University of Paris XI, Dauphine in 1982. He is currently a Research Director at INRIA Sophia-Antipolis in the Computer Vision and Robotics Group. His research interests are in computer vision and image processing and include Image enhancement and Image Restoration, Partial Differential Equations applied to IP and CV, low-level Vision, Self-Calibration, stereo, motion analysis and visual tracking. More generally, he is very interested by the application of mathematics to computer vision and image processing. He has authored and co-authored more than 80 papers. To find out more about his research and some selected publications take a look at <http://www.inria.fr/robotvis/personnel/der/der-eng.html>

**Gilles Aubert** received the Thèse d'Etat es-science Mathématiques from the University of Paris 6, France, in 1986. He is currently Professor at the University of Nice-Sophia Antipolis and member of the J.A Dieudonné Laboratory, Nice, France. His research interests are calculus of variations, nonlinear partial differential equations and numerical analysis; fields of applications include nonlinear elasticity and image processing and in particular: restoration, segmentation, optical flow, reconstruction in medical imaging.